THE JOURNAL OF PHYSICAL CHEMISTRY B
A JOURNAL OF THE AMERICAN CHEMICAL SOCIETY

pubs.acs.org/JPCB

Article

Does Electric Friction Matter in Living Cells?

Published as part of The Journal of Physical Chemistry virtual special issue "Dave Thirumalai Festschrift".

Dmitrii E. Makarov* and Hagen Hofmann*

Cite This: *J. Phys. Chem. B* 2021, 125, 6144–6153

Read Online

ACCESS | Metrics & More | Article Recommendations

ABSTRACT: The thermal motion of charged proteins causes randomly fluctuating electric fields inside cells. According to the fluctuation–dissipation theorem, there is an additional friction force associated with such fluctuations. However, the impact of these fluctuations on the diffusion and dynamics of proteins in the cytoplasm is unclear. Here, we provide an order-of-magnitude estimate of this effect by treating electric field fluctuations within a generalized Langevin equation model with a time-dependent friction memory kernel. We find that electric friction is generally negligible compared to solvent friction. However, a significant slowdown of protein diffusion and dynamics is expected for biomolecules with high net charges such as intrinsically disordered proteins and RNA. The results show that direct contacts between biomolecules in a cell are not necessarily required to alter their dynamics.

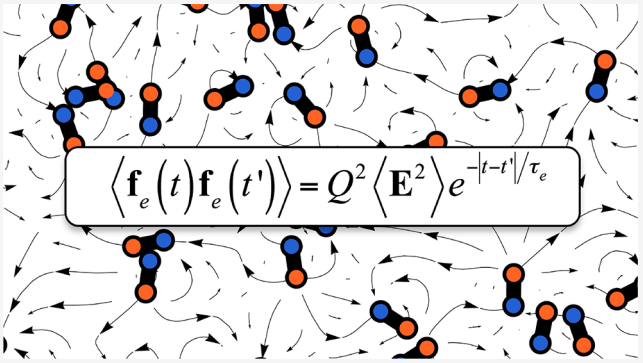

I. INTRODUCTION

The cell is densely filled with proteins, RNAs, and metabolites.[1] Many studies in the past have investigated how the cellular interior affects the stability and dynamics of proteins.[2] Clearly, the excluded volume of numerous intracellular macromolecules (i.e., crowding) can substantially impact the behavior of proteins. In fact, protein concentrations can reach 300 g/L, thus proteins may occupy 30% of the cell volume.[3] As a result, translational diffusion slows down and becomes anomalous,[4] intrinsically disordered proteins (IDPs) become more compact,[5] and folded proteins are expected to be stabilized.[6] Whereas excluded volume crowding has long been the focus of theoretical approaches,[7] other interactions between biomolecules, sometimes called quinary interactions, have received less attention even though they may not be negligible.[3a,8]

Electrostatic interactions are particularly relevant owing to their long-range nature. Given that most biological macromolecules carry charges, we would expect nonspecific electrostatic interactions to play an important role inside cells. In fact, intramolecular charge–charge interactions sensitively alter the conformation of intrinsically disordered proteins (IDPs).[9,10] Electrostatic forces, however, also act on much greater length scales, with consequences for the dynamics of biomolecules. For example, previous simulations found a slowdown in the diffusion of a charged protein in the presence of charged cytosolic biomolecules.[11] Although charge–charge interactions can cause a nonspecific "sticking" of proteins to other cytosolic compounds, here we are concerned with a more general question: do electric field fluctuations caused by cytosolic macromolecules affect the diffusion of a charged particle?

To answer this question, we study the impact of fluctuating electric fields (Figure 1) on the translational diffusion of a charged Brownian particle and on the dynamics of a charged Rouse chain. Following previous approaches,[12] we assume that electric field fluctuations are well-approximated by colored Gaussian noise with a finite correlation time, which is associated with an electric friction memory kernel. Whereas proteins are by far the dominating macromolecules in cells,[1] they carry only moderate net charges on average.[13] Electric friction effects are therefore unlikely to arise from protein net charges. Protein dipole moments, on the other hand, are substantial.[14] The thermally driven tumbling and diffusion of the enormous number of cytosolic proteins therefore appear to be a more likely source of electric friction (Figure 1). Notably, the cytosol also contains significant amounts of RNA,[1] which is highly charged and also has the potential to cause electric friction. However, electric friction due to polyions has been studied previously[12,15] and is not considered in our study.

Received: March 29, 2021
Revised: May 19, 2021
Published: June 3, 2021

https://doi.org/10.1021/acs.jpcb.1c02783
J. Phys. Chem. B 2021, 125, 6144–6153

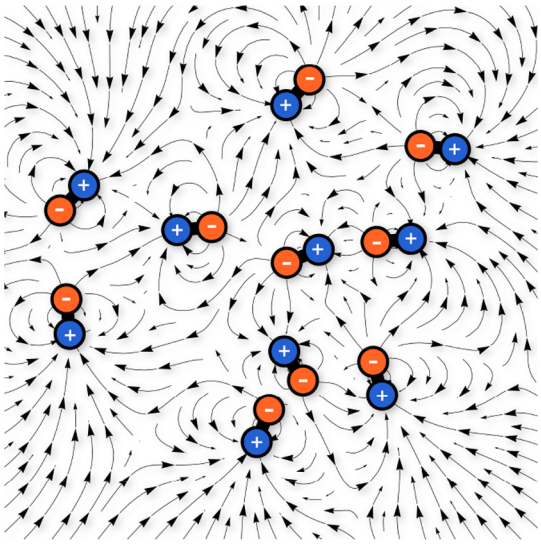

Figure 1. Proteins in the cytosol are diffusing and tumbling dipoles that create a randomly fluctuating electric field. The scheme illustrates the force directions experienced by a charged tracer in a random 2D arrangement of dipoles.

In the following, we derive an explicit expression for the electric friction memory kernel that is caused by randomly orienting protein dipoles. We demonstrate that the slowdown of translational diffusion of a charged tracer protein due to electric friction is generally modest. However, protein tracers with high net charges may be significantly affected by electric friction. In addition, we provide an estimate of how electric friction impacts the conformational dynamics of charged polymers and find that it has similarities to the previously studied internal friction[16] in IDPs.

This article is partitioned into two sections. In section II.A, we introduce a description of electric friction based on a generalized Langevin equation. We derive an expression for the magnitude of the electrostatic force fluctuations and, using the model in which these fluctuations are described as colored noise with a finite correlation time, further derive an expression for the friction memory kernel. We then use these results to estimate how electrostatic fluctuations affect the diffusion coefficients of charged particles. In section II.B, we include electric friction in a Rouse chain and study how it affects the chain reconfiguration time.

II. RESULTS

II.A. Diffusion of a Charged Particle with Electric Friction. In the absence of electric friction (to be considered below), the diffusion of a tracer particle in a liquid can be described by the Langevin equation (LE). Assuming an isotropic and homogeneous medium, it suffices to consider the LE in one dimension

$$m\ddot{x}(t) + \xi_s\dot{x}(t) = f_s(t) \tag{1}$$

Here, $x(t)$ describes the time evolution of the x component of the particle's position, $\dot{x}(t) = v(t) = \mathrm{d}x(t)/\mathrm{d}t$ is the velocity of the particle, m is its mass, ξ_s is the solvent friction coefficient, and $f_s(t)$ is a Gaussian-distributed, delta-correlated random force that satisfies the fluctuation−dissipation theorem

$$\langle f_s(t)\, f_s(t')\rangle = 2k_BT\xi_s\delta(t - t') \tag{2}$$

where k_B is Boltzmann's constant, T is the temperature, and δ is the Dirac delta function. A well-known consequence of eqs 1 and 2 is the Stokes−Einstein relationship that relates the macroscopic drag force characterized by ξ_s to the microscopic diffusion coefficient D via

$$D = \int_0^\infty \langle v(0)\, v(t)\rangle\, \mathrm{d}t = k_BT/\xi_s \tag{3}$$

Randomly tumbling and diffusing proteins in the cytosol will give rise to an additional fluctuating electrostatic force $f_e(t)$, which would have to be added to the rhs of eq 1. According to the fluctuation−dissipation theorem,[17] there is an associated friction force such that the resulting equation of motion is of the form of the generalized Langevin equation[12a] (GLE)

$$m\ddot{x}(t) + \xi_s\dot{x}(t) + \int_{-\infty}^{t} \Gamma(t - \tau)\dot{x}(\tau)\, \mathrm{d}\tau = f_s(t) + f_e(t) \tag{4}$$

Here, the electric friction memory kernel $\Gamma(t)$ satisfies the fluctuation−dissipation theorem

$$\langle f_e(0) f_e(t)\rangle = k_BT\Gamma(t) \tag{5}$$

Importantly, in contrast to solvent friction, which is caused by collisions of solvent molecules with the tracer particle at picosecond time scales, the time scales associated with the tumbling and diffusion of macromolecules are relatively long. As a result, the random force f_e cannot, in general, be viewed as delta-correlated, so the GLE is an integro-differential equation.

If the fluctuations of the electric field $\mathbf{E}$ can be described by a single characteristic time scale τ_e, then its autocorrelation function can be approximated by an exponential function,

$$\langle f_e(0)\, f_e(t)\rangle = \frac{1}{3}Q^2\langle \mathbf{E}^2\rangle \mathrm{e}^{-t/\tau_e} \tag{6}$$

Here, $Q^2\langle \mathbf{E}^2\rangle$ is the mean-squared electrostatic force that acts on a diffusing particle with charge Q. (Note that $\langle \mathbf{E}\rangle = 0$ for a randomly tumbling dipole.) As a result, the friction memory kernel is also an exponential function,

$$\Gamma(t) = \frac{1}{3k_BT}Q^2\langle \mathbf{E}^2\rangle \mathrm{e}^{-t/\tau_e} \tag{7}$$

Given the heterogeneous cytosol composition with macromolecules of different sizes and shapes together with the time scale separation between tumbling and translational motions, this single-exponential approximation is unlikely to be accurate but can easily be generalized to include multiple exponentially decaying terms with different characteristic time scales.[18]

Within the exponential memory kernel approximation, the electric friction is characterized by two parameters: the strength of the electric field fluctuations $\langle \mathbf{E}^2\rangle$ and the memory time τ_e. When the time scale of interest is much longer than τ_e, however, the effect of electric friction can be characterized by a single parameter, the electric friction coefficient

$$\xi_e = \frac{Q^2\langle \mathbf{E}^2\rangle}{3k_BT}\tau_e \tag{8}$$

This parameter corresponds to the Markovian approximation to the GLE, where the friction memory kernel is approximated by the delta function, $\Gamma(t) \approx 2\delta(t)\int_0^\infty \Gamma(\tau)\, \mathrm{d}\tau = 2\xi_e\delta(t)$, and thus the electric friction force in eq 4 is approximated simply by $-\xi_e\dot{x}(t)$. Hence, the friction coefficient defined in eq 8 is usually only meaningful for sufficiently short τ_e. In general, it can be

https://doi.org/10.1021/acs.jpcb.1c02783
J. Phys. Chem. B 2021, 125, 6144−6153

shown that an exponential memory kernel (eq 7) results in a modified Stokes−Einstein relationship, which depends on ξ_e alone and not on τ_e:

$$D = k_B T/(\xi_s + \xi_e) \tag{9}$$

See the Appendix for a derivation of eq 9 from eqs 3, 4, and 7.

To estimate the electric friction memory kernel, we need the magnitude of the electric field fluctuations $\langle \mathbf{E}^2 \rangle$ resulting from the tumbling and diffusion of cytosolic protein dipoles. To compute $\langle \mathbf{E}^2 \rangle$, we consider the electric field produced by a dipole formed by charges $\pm q$ located at $\mathbf{r}_\pm$ and separated by a distance $l = |\mathbf{r}_- - \mathbf{r}_+|$. The electrostatic potential experienced by a charged tracer particle located at the coordinate origin is given by

$$\psi = \frac{q}{C}\left(\frac{e^{-\kappa r_+}}{r_+} - \frac{e^{-\kappa r_-}}{r_-}\right) \approx -\frac{\mathbf{d}}{C}\nabla\left(\frac{e^{-\kappa r}}{r}\right) \tag{10}$$

Here, $r_+ = |\mathbf{r}_+|$ and $r_- = |\mathbf{r}_-|$ are the distances between the diffusing particle and the positively and negatively charged ends of the dipole, respectively, $\mathbf{d} = q(\mathbf{r}_- - \mathbf{r}_+)$ is the dipole moment vector with magnitude $|\mathbf{d}| = d$, κ is the inverse Debye screening length, and $C = 4\pi\epsilon_0\epsilon_w$ with the dielectric constant of water $\epsilon_w = 80$ and the vacuum permittivity ϵ_0. Assuming that the dipole length l is much smaller than the distance r between the dipole and the particle, one finds

$$\psi = \frac{\mathbf{d}\mathbf{r}}{C} K(r) \text{ with } K(r) = (1 + \kappa r)e^{-\kappa r}/r^3 \tag{11}$$

The electric field is $\mathbf{E} = -\nabla\psi$, and its mean-square magnitude $\langle \mathbf{E}^2 \rangle$ is obtained by averaging over all angles θ and positions r, thus leading to

$$\begin{aligned}\langle \mathbf{E}^2 \rangle &= \frac{Nd^2}{C^2}\left\langle K(r)^2 + \frac{r^2}{3}K'(r)^2 + \frac{2}{3}rK'(r)\,K(r)\right\rangle_r \\ &= \frac{4\pi N d^2}{C^2 V}\int_a^R \left[K(r)^2 + \frac{r^2}{3}K'(r)^2 + \frac{2}{3}rK'(r)\,K(r)\right] r^2\,\mathrm{d}r\end{aligned} \tag{12}$$

where the prime indicates the derivative with respect to r (Appendix IV.B). Here, R is the radius of a spherical cell, $V \propto R^3$ is the cell volume, and N is the number of dipoles in a cell. The lower integration bound (a) for the positional distribution must be chosen such that the tracer particle does not collide with the dipole ($a > l/2$); in fact, the dipole approximation used to arrive at eq 11 would even require $a \gg l/2$. To understand how the magnitude of force fluctuations depends on the system size and the dipole concentration, we first consider the case without screening ($\kappa \to 0$) and then discuss the effects at physiological ionic strengths. Under the assumption that the cell is much larger than the dipole, we find

$$Q^2\langle \mathbf{E}^2 \rangle = \frac{8\pi}{3a^3C^2} d^2Q^2c_p \tag{13}$$

for the force fluctuations and

$$Q^2\langle \psi^2 \rangle = \frac{4\pi}{3aC^2} d^2Q^2c_p \tag{14}$$

for the energy fluctuations. Here, $c_p = N/V$ is the concentration of dipoles (proteins) in a cell. Notably, the fluctuation magnitude is independent of the cell size R (which provides a justification of the above spherical symmetry assumption as long as R is large enough) and scales linearly with the concentration of dipoles. Hence, despite the long-range nature of electrostatics, only neighboring dipoles effectively contribute to the force amplitude. In addition, the mean-squared fluctuation amplitude and therefore the electric friction coefficient increase with the squared charge of the tracer particles (Q^2), which may lead to significant contributions for highly charged particles. The expressions in the presence of salt-screening (i.e., at arbitrary κ) are given in Appendix IV.B and were used in all calculations.

With eqs 8 and 12, we can now compute the ratio between electric friction (ξ_e) and solvent friction (ξ_s) for realistic values of c_p, d, and a. A previous study computed the dipole moments of 11 981 proteins from the protein database and obtained a mean dipole moment of 639 D (median = 452).[14] The average size of a bacterial protein is 267 amino acids,[19] which results in a Stokes radius of 2.4 nm using the experimental scaling laws for folded proteins.[20] The dipole length is therefore $l \approx 4.8$ nm, and we took $a = 3l/4$. The protein concentration inside a bacterial cell is ∼6−11 mM (for a randomly tumbling dipole), and we assume a cell volume of 1 fL. Because $\xi_e \propto \tau_e$ (eq 8), we also require the time scale τ_e, which will significantly impact the magnitude of electric friction. The electric field fluctuations at any given point are caused by the rotational and translational motions of the dipoles, and we therefore expect the friction memory kernel (eq 5) to display time scales ranging from those of tumbling (nanoseconds) to diffusion (milliseconds). A conservative estimate would use the lowest possible time scale (dipole tumbling), which is given by $\tau_e \approx \nu\eta/k_BT$ with $\nu \approx (l/2)^3$ for the volume of a dipole with η being the viscosity. We assume that the dipoles tumble independently and experience only the drag force of the solvent that is defined by the viscosity η (1 mPa s). Given these numbers, we find that the relative impact of electric friction decreases drastically with increasing ionic strengths (Figure 2A). For moderately charged particles ($|Q| < 5e$), the electric friction coefficient is several orders of magnitude smaller than solvent friction at physiological ionic strengths (100−300 mM) (Figure 2A). This result is in agreement with the electrostatic energy fluctuations that reach only thermal energy at high net charges (Figure 2B). Given that the net charges of most proteins rarely exceed 5e, we generally conclude that electric friction does not affect the translational motion of proteins significantly. However, highly charged proteins such as histone H1 (net charge +53e) and prothymosin-α (net charge −44e)[21] are likely affected, even at physiological salt concentrations, and their diffusion coefficients can decrease 2-fold (Figure 2C). Importantly, although electric friction seems to be a rather moderate effect compared to other contributions in the cytosol such as direct protein−protein interactions, it should be kept in mind that our results are approximate since the contribution of highly charged RNA as well as fluctuations due to charge regulation[22] such as protonation and deprotonation of ionizable groups were neglected. With these conservative estimates, electric friction is just on the verge of affecting the diffusion of charged proteins in a cell and a more accurate treatment using simulations might discover more pronounced effects. We note that our results can also provide estimates for other scenarios, such as liquid protein condensates with protein concentrations (500 g/L)[23] that even exceed those found in cells.

How can electric friction be identified experimentally? Clearly, disentangling electric friction from other effects such as excluded volume crowding or "sticking" is challenging, yet compared to processes that require direct physical contacts,

https://doi.org/10.1021/acs.jpcb.1c02783
J. Phys. Chem. B 2021, 125, 6144−6153

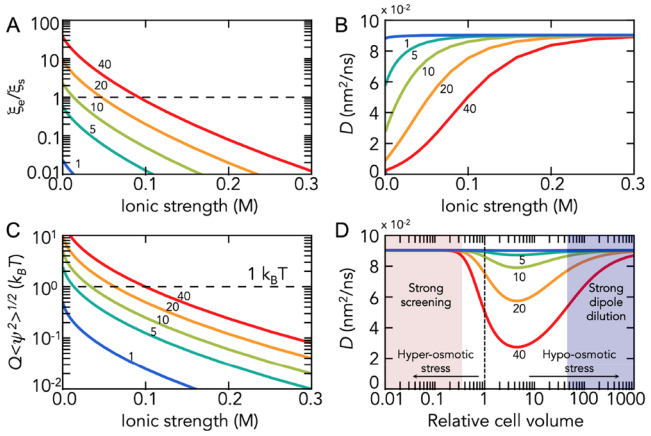

Figure 2. Effect of electric friction on the diffusion of a charged particle (net charge number indicated). (A) The electric friction coefficient (ξ_e) relative to solvent friction (ξ_s), (B) the diffusion coefficient, and (C) the energy magnitude of electrostatic fluctuations are moderately impacted for diffusing particles with a net charge of $Q < 5e$. Significant effects on particle diffusion at physiological ionic strengths (0.1−0.3 M) are observed only for highly charged particles. Calculations were performed with the following parameters: $c_p = 6$ mM, $a = 3/4\ l$, $l = 4.8$ nm, and $d = 635$ D. (D) A change in cell volume simultaneously changes the ionic strength and dipole concentration. At low cell volumes (i.e., high ionic strength and dipole concentration, red area) and high cell volumes (i.e., low ionic strength and low dipole concentrations, blue area), the effect of electric friction is negligible. In the intermediate regime, we would expect a slowdown of the diffusion of a charged tracer particle if the cell volume increases compared to its natural value ($V = 1$).

electric friction has an unusual dependence on the cell volume within the limit given by our assumption of a fixed time scale of electric field fluctuations. Although electric friction does not explicitly depend on the volume of a cell, altering the cellular volume by applying osmotic stress will alter the concentration of protein dipoles (eq 13) together with the ionic strength of the cellular interior. Clearly, in the extreme case of strong dilution (Figure 2D) (i.e., at large cell volumes), electric friction is negligible. Remarkably, the same phenomenon is observed at extremely small cell volumes (Figure 2D). Although both dipole concentration and ionic strength are high at small cell volumes, the high ionic strength effectively screens charge interactions such that electric friction remains marginal. In the intermediate regime, electric friction has a maximum. Particularly for the reported cellular concentrations of proteins (6 mM) and ionic strength (0.15 M), a 2-fold increase in cell volume would cause an increase in electric friction (i.e., a decrease of the diffusion coefficient of a charged tracer particle (Figure 2D)). On the contrary, excluded volume effects and/or direct interactions of the particle with cytosolic components would rather cause a slowdown in diffusion. Recent measurements by König et al. indeed found a slowdown in the translational diffusion of a charged disordered protein under hyperosmotic conditions,[24] which would suggest that crowding and "sticking" dominate inside cells. We note, however, that our estimate for the volume dependence of electric friction is valid only under the assumption that the time scale of electric field fluctuations (τ_e) is invariant under volume changes. Clearly, a dipole in a cell experiences the field of neighboring protein dipoles such that volume changes will also affect the average tumbling time.

II.B. Rouse Chain with Electric Friction. The internal dynamics of proteins (i.e., their conformational changes) cover many orders of magnitude in time, from the reconfiguration time scales in unfolded proteins to those of protein folding and large molecular assemblies.[25] Because proteins function in aqueous solutions, frictional forces determine not only their translational diffusion but also their internal dynamics such as folding. Theories based on Kramers' model of diffusive barrier crossing[26] in the overdamped limit predict a direct proportionality between the folding time τ and viscosity ($\tau \propto \eta$),[27] which has indeed been observed for the millisecond folding dynamics of two-state proteins.[28] In contrast, deviations from this behavior were found for proteins that fold within microseconds[29] or that exhibit significant ruggedness in their energy landscapes.[27b] Two alternative ways of analyzing these experimental data have been used in the past. Either a friction component resulting from interactions within the protein has been invoked, which leads to an additive time scale that is independent of the viscosity of the solvent,[27b,29a] or if a scaling relationship between the reaction time and solvent viscosity is assumed, then a weaker viscosity dependence such as $\tau \propto \eta^{\beta}$ with $\beta < 1$ was used to describe the experimental data.[30] Indeed, such fractional viscosity dependencies have been identified for the diffusion of small molecular compounds[31] and the internal dynamics of molecules.[32] Physical interpretations of such behaviors range from a viscosity-dependent change in the hydrodynamic coupling between the solvent and the molecule[33] and a breakdown of continuum hydrodynamics due to the finite size of the solvent molecules[31a,34] to memory effects caused by solvent relaxation or degrees of freedom different from the probed reaction coordinate.[32,35] Non-Markovian electric friction may also contribute to the complexity of the observed internal dynamics of charged biopolymers.

Thus motivated, we seek to understand the effect of electric friction on the internal dynamics of charged biopolymers. To this end, we consider the dynamics of the simplest polymer model, a Rouse chain. Despite their simplicity, Rouse/Zimm-type models often offer a quantitative description of reconfiguration dynamics of intrinsically disordered proteins[16,36] and other biopolymers.[37] Their success is in part due to the fact that they are coarse-grained models capturing specific intermonomer interactions via a few adjustable parameters. Here, for simplicity, we focus on the Rouse model, which ignores hydrodynamic interactions. The usual coarse-graining monomeric unit of the Rouse chain is the Kuhn segment chosen to be sufficiently large such that adjacent Kuhn segments are statistically independent. In the present case, however, it is essential to consider another length scale l_C, which is the length over which the spatial correlations of the electric field acting on the polymer decay. If l_C is comparable to or smaller than the size of the Kuhn segment, then the electric forces acting on each Kuhn segment are statistically independent. Is this a reasonable assumption?

When taking the nearest-neighbor distance[38] between two dipoles as an upper limit for l_C, we find 3−3.4 nm at cellular concentrations (6−11 mM) (i.e., much larger than the Cα distance between adjacent amino acids (0.38 nm) and also larger than the Kuhn length (0.55 nm) of polypeptide chains).[39] Hence, neighboring amino acids will experience the same electrostatic force.

When l_C exceeds the size of the Kuhn segment but is still much smaller than the radius of gyration of the entire chain, R_g, then it is expedient to further coarse grain the chain to de Gennes "blobs" of size l_C. Because of the self-similarity of the Rouse model, such coarse graining does not affect the model's dynamic properties (except for short time scales), yet now the electric

https://doi.org/10.1021/acs.jpcb.1c02783
J. Phys. Chem. B 2021, 125, 6144−6153

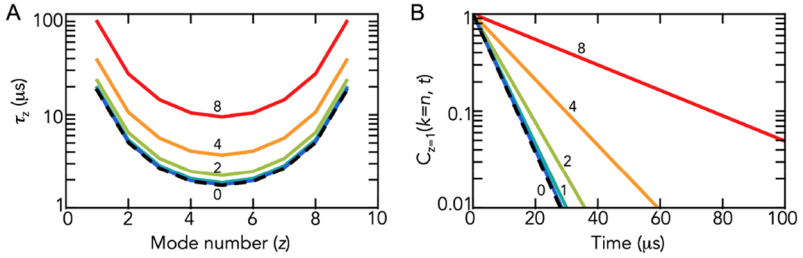

Figure 3. Effect of electric friction on the reconfiguration dynamics of a Rouse chain. (A) Mode spectrum of a chain with $n = 10$ blobs and a blob size of 100 monomers. Mode number z is given by $z = nq/2\pi$ at increasing net charges of the chain monomers (indicated). The spectrum for an uncharged Rouse chain is shown as a black dashed line. (B) Mode-specific end-to-end vector correlation function ($z = 1$) with $n = 10$ at increasing net charges of the chain beads (indicated). The color code is identical to that in A.

forces acting on each blob may be considered statistically independent. This case is discussed in detail below. If, however, l_C is comparable to or greater than R_g, then electric forces on all monomers of the chain are correlated. It is then instructive to consider the limit in which all monomers feel the same electric field. Interestingly, unless the chain is charged uniformly, interaction with the electric field also leads to friction. This case is discussed at the end of this section and in Appendix D.

Consider the case $l_C \ll R_g$ and assume that the problem is adequately course-grained such that the electric forces on each monomeric unit are statistically independent of one another. The chain is then treated as a Rouse chain (i.e., as a string of n harmonically coupled beads (blobs)).[40] A Rouse model with explicit noncovalent contacts between beads has been developed by Barsegov, Morrison, and Thirumalai[41] but since we mainly focus on interactions of the beads with external electric fields, we implicitly account for electrostatic interactions between chain beads by the spring constant of the interbead interaction (which may depend on the ionic strength). In addition to the solvent friction (and the associated delta-correlated random force), each bead also experiences an electric friction force along with the stochastic force caused by the fluctuations in the electric field. These forces depend on the charges of each bead, and in general, a numerical solution of the problem can be obtained for any given value of such charges. To ensure that the problem is tractable analytically, however, here we will consider the case in which all of the monomer charges are the same.

The equation of motion for the x coordinate of the kth bead is thus given by the GLE (cf. eq 4) with two modifications. First, it now includes the interaction force between the beads, and second, we (conventionally) neglected the inertia of the beads that is important only at very short time scales.[42] The resulting overdamped GLE is

$$\xi_s \dot{x}(k, t) + \xi_e \tau_e^{-1} \int_{-\infty}^{t} \dot{x}(k, \tau) e^{-|t-\tau|/\tau_e} d\tau + \gamma[2x(k, t) - x(k-1, t) - x(k+1, t)] = f_s(k, t) + f_e(k, t) \quad (15)$$

Here, the spring constant (γ) is given by

$$\gamma = 3nkT/\langle r_{chain}^2 \rangle \quad (16)$$

where $\langle r_{chain}^2 \rangle$ is the mean square end-to-end distance of the chain.[16a] Importantly, eq 15 is not specific to electric friction. Any fluctuating noise source with an exponentially decaying memory kernel will lead to the same formulation, and the following conclusions are general.

We are interested in computing the average reconfiguration time of the chain. Following previous approaches,[16,42] we define this reconfiguration time by the correlation function $C_k(t)$ of the vector that connects a bead at position 0 with another bead at position k

$$C(k, t) = 3\langle [x(k, t) - x(0, t)][x(k, 0) - x(0, 0)] \rangle \quad (17)$$

The mean reconfiguration time of the chain is given by

$$\tau_k = \frac{\int_0^\infty tC(k, t)\, dt}{\int_0^\infty C(k, t)\, dt} \quad (18)$$

After switching from bead numbers (k) to modes (q) using Fourier transform (i.e., neglecting effects from the chain termini), eq 15 becomes

$$\xi_s \dot{x}(q, t) + \xi_e \tau_e^{-1} \int_{-\infty}^{t} \dot{x}(q, t) e^{-|t-\tau|/\tau_e} d\tau + 2\gamma(1 - \cos q)\, x(q, t) = f_s(q, t) + f_e(q, t) \quad (19)$$

Here, $q = 2\pi\{0, 1, 2, \ldots\}/n$ for a periodic chain. The solution is obtained after reducing eq 19 to a second-order differential equation and using time Fourier transform (Appendix IV.C)

$$\hat{x}(q, \omega) = \frac{(1 - i\omega\tau_e)[\hat{f}_s(q, \omega) + \hat{f}_e(q, \omega)]}{-\xi_s\omega(i + \tau_e\omega) - i\omega\xi_e + 2\gamma(1 - \cos q)(1 - i\omega\tau_e)} \quad (20)$$

In contrast to a Rouse chain, the introduction of colored noise results in two relaxation times (τ_1 and τ_2) that are given by the two eigenvalues (ω_1 and ω_2) of eq 20

$$\omega_{1,2} = -i(M \pm \sqrt{M^2 - L})/2\xi_s\tau_e = -i/\tau_{1,2} \quad (21)$$

with $M = \xi_s + \xi_e + 2\gamma\tau_e(1 - \cos q)$ and $L = 8\xi_s\tau_e\gamma(1 - \cos q)$. Using eq 20 together with the fluctuation dissipation theorems (Appendix IV.C), the correlation function is

$$C(k, t) = \frac{3k_BT}{\xi_s\tau_e^2} \sum_q A(q, k)\, C_q(t) \text{ with } A(q, k) = 2(1 - \cos kq) \quad (22)$$

and the mode number is z. The mode-specific correlation function in eq 22 is a double-exponential function given by

$$C_q(t) = \frac{\tau_1\tau_2}{(\tau_1 - \tau_2)(\tau_1 + \tau_2)}[\tau_2(\beta\tau_1^2 - \tau_e^2)e^{-t/\tau_1} - \tau_1(\beta\tau_2^2 - \tau_e^2)e^{-t/\tau_2}] \quad (23)$$

Here, τ_e is the tumbling time of the dipoles as defined in section A and $\beta = 1 + \xi_e/\xi_s$. Using eqs 18 and 23, we arrive at the average mode-dependent relaxation time of the chain

https://doi.org/10.1021/acs.jpcb.1c02783
J. Phys. Chem. B 2021, 125, 6144−6153

$$\tau_q = \tau_2 + \frac{\tau_1^2 - \beta^{-1}\tau_e^2}{\tau_1 + \tau_2} = \frac{\xi_s}{\gamma q^2} + \frac{\xi_e}{\gamma q^2} + \frac{\xi_e \tau_e}{\xi_s + \xi_e} \quad (24)$$

where we used $(1 - \cos q) \approx q^2/2$. In the limit of the vanishing electric friction (i.e., $\xi_e \to 0$), we find $\tau_q = \xi_s/\gamma q^2$, which is the relaxation time scale spectrum of the classical Rouse model without electric friction. Notably, the additional friction component adds two contributions to the standard Rouse mode relaxation times. The first component is mode-dependent (second term in eq 24), and the other component contributes equally to all modes (third term in eq 24). These two contributions are also of interest for understanding internal friction processes in polymers. For example, conflicting observations have been reported for the mode dependence of internal friction.[16a] Whereas single-molecule FRET experiments were in agreement with a mode-independent contribution of internal friction,[16b] experiments on long polymers suggest a mode dependence of internal friction.[43] Equation 24 combines both types of contributions. In particular, term q^{-2} is proportional to the length of the chain squared (n^2) such that the second term in eq 24 will dominate for long chains whereas the mode-independent term (third term) is more important for short chains.

In the specific case of electric friction considered here, the additional friction component causes a slowdown of the chain dynamics across the whole mode spectrum (Figure 3A). In addition, the correlation functions have two decay components, both of which depend on electric friction (eq 21). Yet, the slower component (τ_2) dominates the correlation function, thus causing a nearly exponential decay (Figure 3B).

Now consider the limit $l_C \gg R_g$. In this case, all monomers of the chain will experience the same external electric field. For a uniformly charged chain, this fluctuating field will alter the center-of-mass diffusion of the chain, as described in section II.A, but the internal dynamics of the chain will remain unaffected. Notably, this is not the case if the chain monomers carry different charges. It can be shown (Appendix IV.D) that friction forces analogous to eq 7 arise under these conditions. The resulting GLEs for the chain are more complicated than eq 15 in that they exhibit hydrodynamic-like coupling between monomers, where the friction force on a given monomer depends on the velocity histories of other monomers. For a given nonuniform charge distribution along the chain, these equations in general require a numerical solution.

In general, the overall strength of electric friction from dipole tumbling remains moderate for intrinsically disordered proteins. Clearly, this might change if all sources of electric field fluctuations inside a cell are taken into account.

III. CONCLUSIONS

The variety of intermolecular interactions between macromolecules in the cellular interior is enormous, ranging from simple excluded volume to hydrophobic sticking to electrostatic effects. Here, we studied the effects of long-range electrostatic forces (as opposed to forces arising from direct physical contacts between macromolecules) on the diffusive dynamics of biopolymers. We described the complex cytosolic mixture of crowding proteins as a collection of diffusing and tumbling dipoles that cause a fluctuating electric field inside the cell. We obtained an analytical estimate of the magnitude of such field fluctuations and how these fluctuations impact the diffusion of a charged particle and the dynamics of a charged Rouse chain. To keep the problem analytically tractable, we treated electric field fluctuations as colored noise with a single characteristic time scale and an exponential memory kernel. The time scale is determined by the tumbling time of the dipoles. We show that the resulting friction coefficient is independent of the system size and proportional to the concentration of dipoles (i.e., the protein concentration in the cytosol). The friction coefficient also increases with the squared net charge of a diffusing particle, which causes a prominent slowdown in diffusion for highly charged particles. Similar effects were also found when investigating the behavior of a chain of charged beads in such a field. We find a significant effect of electric friction only if the net charge of the chain monomers exceeds an absolute charge of 10e.

Our numerical results provide only a crude estimate of electric friction effects. In reality, electrostatic fluctuations occur at multiple time scales and are caused not only by tumbling protein dipoles but also by other charged macromolecules such as RNA, charge regulation processes such as protonation and deprotonation of ionizable groups, and the translational diffusion of all charged species in the cytosol. However, our main goal was to provide an analytical framework to estimate electric friction. Our approach of describing the effect of electric field fluctuations on the diffusion of charged particles using GLEs is sufficiently flexible to account for additional noise sources. However, precise values for the strength of these fluctuations in realistic compositions of the cytosol are better obtained from molecular simulations.[11] Our results suggest that even with the conservative estimate made in this work, electric friction in cells is on the verge of impacting the diffusion of highly charged particles and polymers without direct physical contacts.

IV. Appendix

IV.A. Diffusion in the Presence of Electric Friction. To obtain the Stokes−Einstein relationship for the diffusion of a particle in the presence of white and colored noise, we write eq 4 in terms of velocities

$$m\dot{v}(t) + \xi_s v(t) + \xi_e \tau_e^{-1} \int_{-\infty}^{t} v(t) e^{-|t-\tau|/\tau_e} d\tau = f_s(t) + f_e(t) \quad (A1)$$

Using integration by parts, we obtain

$$m\dot{v}(t) + \xi_s v(t) + \xi_e v(t) - \xi_e \tau_e^{-1} \int_{-\infty}^{t} \dot{v}(t) e^{-|t-\tau|/\tau_e} d\tau = f_s(t) + f_e(t) \quad (A2)$$

To remove the integral, we multiply eq A2 by $\tau_e\, \partial/\partial t$ and add the result to eq A2, which reduces the integrodifferential equation to a second-order differential equation

$$\tau_e m\ddot{v}(t) + [m + \tau_e(\xi_s + \xi_e)]\dot{v}(t) + (\xi_s + \xi_e)v(t) = \dot{f}_s(t) + \tau_e \ddot{f}_s(t) + f_e(t) + \tau_e \dot{f}_e(t) \quad (A3)$$

Using the Fourier transform ($t \to \omega$) defined by $\hat{v}(\omega) = \frac{1}{2\pi}\int_{-\infty}^{\infty} v(t) e^{i\omega t}\, d\omega$, we obtain the solution

$$\hat{v}(\omega) = \frac{(1 - i\omega\tau_e)[\hat{f}_s(\omega) + \hat{f}_e(\omega)]}{-\omega^2\tau_e - i\omega[m + \tau_e(\xi_s + \xi_e)] + (\xi_s + \xi_e)} = G(\omega)[\hat{f}_s(\omega) + \hat{f}_e(\omega)] \quad (A4)$$

https://doi.org/10.1021/acs.jpcb.1c02783
J. Phys. Chem. B 2021, 125, 6144−6153

with the two Eigenvalues $\omega_1 = -i/\tau_e$ and $\omega_2 = -i(\xi_s + \xi_e)/m$ and the diffusion time scale $\tau_D = m/(\xi_s + \xi_e)$. The Green−Kubo relationship (eq 3) is then given by

$$\langle v(t)v(0)\rangle = \int\int_{-\infty}^{\infty} \hat{v}(\omega)\,\hat{v}(\omega')e^{-i\omega t}\,d\omega\,d\omega' \tag{A5}$$

The fluctuation−dissipation theorems after Fourier transform are given by $\langle \hat{f}_s(\omega)\hat{f}_s^*(\omega')\rangle = \frac{k_BT}{\pi}\xi_s\delta(\omega-\omega')$ and $\langle \hat{f}_e(\omega)\hat{f}_e^*(\omega')\rangle = \frac{k_BT}{\pi}\frac{\xi_s}{1+\omega^2\tau_e^2}\delta(\omega-\omega')$ where the asterisk indicates the complex conjugate. With eq A4 and the identity $f(\omega) \equiv f^*(-\omega)$, we then obtain for the velocity autocorrelation function

$$\langle v(t)\,v(t')\rangle = \frac{k_BT\xi_s}{\pi}\int\int_{-\infty}^{\infty} G(\omega)\,G(\omega')\,\delta(\omega+\omega')e^{-i\omega t}\,d\omega\,d\omega' + \frac{k_BT\xi_e}{\pi}\int\int_{-\infty}^{\infty}\frac{G(\omega)\,G(\omega')}{1+\omega^2\tau_e^2}\delta(\omega+\omega')e^{-i\omega t}\,d\omega\,d\omega' \tag{A6}$$

Solving the integrals gives

$$\langle v(t)v(t')\rangle = \frac{k_BT}{m^2}\left\{\xi_s\tau_D e^{-t/\tau_D} + \xi_e\frac{\tau_D}{\tau_e^2-\tau_D^2}[\tau_e e^{-t/\tau_e} - \tau_D e^{-t/\tau_D}]\right\} \tag{A7}$$

which results in the modified Stokes−Einstein relationship by inserting this expression into eq 3.

IV.B. Electrostatic Dipole Potential with Salt Screening. Starting with eq 11, we can write the electric field for a single dipole

$$\mathbf{E} = -\nabla\psi = \frac{1}{C}[-\mathbf{d}K(r) - (\mathbf{dn})rK'(r)\mathbf{n}] \tag{B1}$$

where $\mathbf{n} = \nabla r = \mathbf{r}/r$ is the vector of unit length connecting the center of the dipole with the diffusing particle. From eq B1, it is easy to see that by averaging over the dipole orientation we obtain $\langle \mathbf{d}\rangle = \mathbf{0}$ and therefore $\langle \mathbf{E}\rangle = \mathbf{0}$. To compute the mean-squared fluctuation, we compute $\mathbf{E}^2$

$$\mathbf{E}^2 = \frac{1}{C^2}\{-\mathbf{d}^2K(r)^2 - (\mathbf{dn})^2[r^2K'(r)^2 + 2rK'(r)K(r)]\} \tag{B2}$$

Finally, with $\mathbf{d}^2 = d^2$ and the angular average $\langle \mathbf{dn}\rangle = d^2/3$, we obtain the expression in eq 12 by multiplying by the number of independent dipoles N. When performing the average in eq 12, we obtain for $R^3 \gg a^3$

$$Q^2\langle \mathbf{E}^2\rangle = \frac{2\pi}{3C^2a^3}d^2Q^2c_p e^{-2a\kappa}(4 + 8a\kappa + 4a^2\kappa^2 + a^3\kappa^3) \tag{B3}$$

Similarly, we obtain for the mean-square fluctuations of the electrostatic energy with $R \gg a$

$$Q^2\langle \psi^2\rangle = \frac{2\pi}{3C^2a}d^2Q^2c_p e^{-2a\kappa}(2 + a\kappa) \tag{B4}$$

IV.C. Rouse Chain in the Presence of Electric Friction. We start with the fluctuation dissipation theorems for the two different noise processes.

$$\langle f_s(k,t)\,f_s(k',t')\rangle = 2k_BT\xi_s\delta(t-t')\,\Delta(k-k') \tag{C1}$$

$$\langle f_e(k,t)f_e(k',t')\rangle = k_BT\xi_e\frac{e^{-|t-t'|/\tau_e}}{\tau_e}\Delta(k-k') \tag{C2}$$

Here, eq C1 accounts for the random force exerted by the solvent and eq C2 accounts for the fluctuations of the electrostatic force, which are assumed to have a characteristic time scale of τ_e. Symbols δ and Δ are the Dirac and Kronecker delta functions, respectively. Note that the solvent and electrostatic random forces, $f_s(k, t)$ and $f_e(k', t')$, are assumed to be statistically independent

It is convenient to adopt periodic boundary conditions (i.e., $x(n+k,t) \equiv x(k,t)$).[16a,44] After multiplying both sides of eqs C1 and C2 by e^{iqk} and summing over k, we obtain

$$\langle f_s(q,t)\,f_s(q',t')\rangle = 2nk_BT\xi_s\delta(t-t')\,\Delta(q-q') \tag{C3}$$

$$\langle f_e(q,t)\,f_e(q',t')\rangle = nk_BT\xi_e\frac{e^{-|t-t'|/\tau_e}}{\tau_e}\Delta(q-q') \tag{C4}$$

which can also be written as

$$\langle f_s(q,t+t')\,f_s(q',t')\rangle = 2nk_BT\xi_s\delta(t)\,\Delta(q-q') \tag{C5}$$

$$\langle f_e(q,t+t')\,f_e(q',t')\rangle = nk_BT\xi_e\frac{e^{-|t|/\tau_e}}{\tau_e}\Delta(q-q') \tag{C6}$$

By multiplying both sides of eqs C5 and C6 by $e^{-i\omega t'}e^{i\omega(t+t')}$ and integrating over t and t', we obtain the time Fourier transforms

$$\langle \hat{f}_s(q,\omega)\hat{f}_s^*(q',\omega')\rangle = \frac{nk_BT}{\pi}\xi_s\delta(\omega-\omega')\,\Delta(q-q') \tag{C7}$$

$$\langle \hat{f}_e(q,\omega)\hat{f}_e^*(q',\omega')\rangle = \frac{nk_BT}{\pi}\frac{\xi_s}{1+\omega^2\tau_e^2}\delta(\omega-\omega')\,\Delta(q-q') \tag{C8}$$

After reducing eq 19 to a second-order differential equation (Appendix A), we obtain

$$\xi_s[\dot{x}(q,t) + \tau_e\ddot{x}(q,t)] + \xi_e\dot{x}(q,t) + 2\gamma(1-\cos q)[x(q,t) + \tau_e\dot{x}(q,t)] = f_s(q,t) + \tau_e\dot{f}_s(q,t) + f_e(q,t) + \tau_e\dot{f}_e(q,t) \tag{C9}$$

Using time Fourier transform, we obtain eq 20 in the main text, which can be rewritten in terms of eigenvalues ω_1 and ω_2 as

$$\hat{x}(q,\omega) = G(q,\omega)[\hat{f}_s(q,\omega) + \hat{f}_e(q,\omega)] \tag{C10}$$

with $G(q,\omega) = -\frac{1+i\omega\tau_0}{\xi_s\tau_e(\omega-\omega_1)(\omega-\omega_2)}$ and $G(-q,-\omega) = -\frac{1-i\omega\tau_0}{\xi_s\tau_e(\omega-\omega_1^*)(\omega-\omega_2^*)}$. The end-to-end vector correlation function is defined by

$$C(k,t) = 3\langle[x(k,t) - x(0,t)][x(k,0) - x(0,0)]\rangle \tag{C11}$$

and using the definitions of Fourier transform we rewrite eq C11 as

https://doi.org/10.1021/acs.jpcb.1c02783
J. Phys. Chem. B 2021, 125, 6144−6153

$$C(k,t) = 3n^{-2}\sum_{q}\sum_{q'}(e^{-iqk}-1)(e^{-iq'k}-1)\int\int_{-\infty}^{\infty}\hat{x}(q,\omega)\,\hat{x}(q',\omega')e^{-i\omega t}\,d\omega\,d\omega' \quad (C12)$$

With the two noise processes (eqs C7 and C8) and the solutions (eq C10), we finally obtain

$$C(k,t) = \frac{3k_BT\xi_s}{n}\sum_{q,q'}(e^{-iqk}-1)(e^{-iq'k}-1)\left\{\int\int_{-\infty}^{\infty}G(q,\omega)G(q',\omega')\delta(\omega-\omega')e^{-i\omega t}\,d\omega\,d\omega' + \frac{\xi_e}{\xi_s}\int\int_{-\infty}^{\infty}\frac{G(q,\omega)G(q',\omega')}{1+\omega^2\tau_e^2}\delta(\omega-\omega')e^{-i\omega t}\,d\omega\,d\omega'\right\} \quad (C13)$$

Integration over ω' and the summation of q' gives, together with the definitions of $G(q,\omega)$ and $G(-q,-\omega)$,

$$C(k,t) = \frac{3k_BT}{\pi\xi_s\tau_e^2}\sum_{q}2(1-\cos qk)\left\{\int_{-\infty}^{\infty}\frac{(1-i\omega\tau_e)(1+i\omega\tau_e)e^{-i\omega t}}{(\omega-\omega_1)(\omega-\omega_1^*)(\omega-\omega_2)(\omega-\omega_2^*)}\,d\omega + \frac{\xi_e}{\xi_s}\int_{-\infty}^{\infty}\frac{(1-i\omega\tau_e)(1+i\omega\tau_e)e^{-i\omega t}}{(1+\omega^2\tau_e^2)(\omega-\omega_1)(\omega-\omega_1^*)(\omega-\omega_2)(\omega-\omega_2^*)}\,d\omega\right\} \quad (C14)$$

By solving the integrals and substituting $\tau_j = -i/\omega_j$ with $j = \{1, 2\}$, we obtain

$$C(k,t) = \frac{3k_BT}{\xi_s\tau_e^2}\sum_{q}2(1-\cos kq)\left\{\frac{\tau_1\tau_2}{(\tau_1-\tau_2)(\tau_1+\tau_2)}[\tau_2(\beta\tau_1^2-\tau_e^2)e^{-t/\tau_1}-\tau_1(\beta\tau_2^2-\tau_e^2)e^{-t/\tau_2}]\right\} = \frac{3k_BT}{\xi_s\tau_e^2}\sum_{q}2(1-\cos kq)C_q(k,t) \quad (C15)$$

with $\beta = 1 + \xi_e/\xi_s$.

IV.D. Charged Rouse Chain in the Limit of Large Electric Field Correlation Lengths. We start by noting that the GLE (eq 4) can be derived from a "microscopic" model, in which coordinate x is coupled, via a Hookean spring, to a single fictitious overdamped "bath" degree of freedom y.[45] The combined 2D system (x, y) undergoes Langevin dynamics without memory, but once y has been integrated out of the problem, the resulting dynamics of x alone obeys the GLE. Similarly, eq 15 can be derived by introducing a set of bath degrees of freedom $y(k)$, with each harmonically coupled to the corresponding monomer coordinate $x(k)$. Surrogate coordinates $y(k)$ represent the degrees of freedom of the surroundings that couple to the chain via electrostatic forces.

When each monomer feels the same electric field, then their coordinates must couple to a single surrogate degree of freedom y, and the potential energy of the system is given by

$$U = U_R[x(1),\cdots,x(n)] + \sum_{k=1}^{n}\gamma_0[c_kx(k)-y]^2/2 \quad (D1)$$

where U_R is the usual quadratic potential of the Rouse chain, γ_0 is a coupling spring constant, and c_k is a dimensionless coefficient that quantifies the relative coupling of each bead to the electric field, which depends on the bead's charge. Parameters γ_0 and c_k will be related to the magnitude of the electric field fluctuations and to the monomer charges below.

The equations of motion for the combined system are the coupled Langevin equations

$$\xi_s\dot{x}(k) = -\frac{\partial U}{\partial x(k)} + f_s(k) = -\frac{\partial U_R}{\partial x(k)} - c_k\gamma_0\left[\sum_{l=1}^{n}c_jx(j) - y\right] + f_s(k) \quad (D2)$$

and

$$\xi_y\dot{y} = -\frac{\partial U}{\partial y} + f_y(k) = \gamma_0\left[\sum_{l=1}^{n}c_jx(j) - y\right] + f_y \quad (D3)$$

where ξ_y is a friction coefficient and f_y is the associated random noise for auxiliary mode y. Similar to the procedure described in ref 45, variable y can be integrated out of the problem, resulting in a system of coupled GLEs for the chain monomers

$$\xi_s\dot{x}(k,t) = -\frac{\partial U_R}{\partial x(k)} - \sum_{l=1}^{n}\int_0^t\Gamma_{kl}(t-t')\dot{x}_l(j)\,dt' + \psi(k,t) \quad (D4)$$

where $\psi(k,t)$ is a random force with a zero mean that satisfies the fluctuation−dissipation relationship

$$\langle\psi(k,t)\,\psi(l,t')\rangle = k_BT\Gamma_{kl}(t-t') + 2\xi_s\delta(t-t') \quad (D5)$$

and

$$\Gamma_{kl}(t) = \gamma_0c_kc_le^{-|t|/\tau_e} \quad (D6)$$

is the matrix of the friction kernels, with the memory time τ_e that can be expressed in terms of the parameters of the problem:

$$\tau_e = \xi_y/\gamma_0 \quad (D7)$$

Notice that if $\Gamma_{kl}(t) \to 0$ for $k \neq l$, then the Rouse model (eq 15) is recovered. Since the quantity $k_BT\Gamma_{kk}(0)$ is the mean squared amplitude of the electrostatic force acting on the kth charge (whose value we call Q_k), we can write $k_BT\Gamma_{kk}(0) = \frac{\langle E^2\rangle Q_k^2}{3}$, and thus we can rewrite eq D6 as

$$\Gamma_{kl}(t) = \frac{Q_kQ_l\langle E^2\rangle}{3k_BT}e^{-|t|/\tau_e} \quad (D8)$$

a result similar to eq 7, which expresses the memory kernels entering eq 4 in terms of the physical parameters of the chain and its surroundings.

For any specified set of charges Q_k, finding the relaxation modes of the coupled equations of motion (eq D4 or, equivalently, finding the normal Langevin modes of eqs D2 and D3) can be accomplished numerically by reducing this to a linear algebra problem.[46]

If all monomer charges are identical, $Q_k = Q$, then the memory kernels $\Gamma_{kl}(t) = \frac{Q^2\langle E^2\rangle}{3k_BT}e^{-|t|/\tau_e}$ are identical for any k and l, and thus the friction forces felt by each monomer are also identical. The equations of motion for any relative distance $x_k - x_l$ thus do not contain an electric friction, and thus this friction does not have any effect on the polymer's internal dynamics. This conclusion is of course obvious: since all monomers feel exactly the same external force at any point of time, this force, while

https://doi.org/10.1021/acs.jpcb.1c02783
J. Phys. Chem. B 2021, 125, 6144−6153

altering the motion of the chain's centroid, has no effect on its internal dynamics.

AUTHOR INFORMATION

Corresponding Authors

Dmitrii E. Makarov − *Department of Chemistry and Oden Institute for Computational Engineering and Sciences, University of Texas at Austin, Austin, Texas 78712, United States;* orcid.org/0000-0002-8421-1846; Email: makarov@cm.utexas.edu

Hagen Hofmann − *Department of Chemical and Structural Biology, Weizmann Institute of Science, 76100 Rehovot, Israel;* orcid.org/0000-0003-1669-3158; Email: hagen.hofmann@weizmann.ac.il

Complete contact information is available at: https://pubs.acs.org/10.1021/acs.jpcb.1c02783

Notes

The authors declare no competing financial interest.

ACKNOWLEDGMENTS

This research was supported by the Robert A. Welch Foundation (grant no. F-1514 to DEM), the U.S. National Science Foundation (grant no. CHE 1955552 to D.E.M.), the Israel Science Foundation (grant no. ISF 2253/18 to H.H.), the Benoziyo Fund for the Advancement of Science, the Carolito Foundation, the Gurwin Family Fund for Scientific Research, the Leir Charitable Foundation, and the Koshland family (H.H.).

REFERENCES

(1) Theillet, F.-X.; Binolfi, A.; Frembgen-Kesner, T.; Hingorani, K.; Sarkar, M.; Kyne, C.; Li, C.; Crowley, P. B.; Gierasch, L.; Pielak, G. J.; Elcock, A. H.; Gershenson, A.; Selenko, P. Physicochemical properties of cells and their effects on intrinsically disordered proteins (IDPs). *Chem. Rev.* **2014**, *114* (13), 6661−6714.

(2) (a) Ebbinghaus, S.; Dhar, A.; McDonald, J. D.; Gruebele, M. Protein folding stability and dynamics imaged in a living cell. *Nat. Methods* **2010**, *7*, 319. (b) Davis, C. M.; Gruebele, M.; Sukenik, S. How does solvation in the cell affect protein folding and binding? *Curr. Opin. Struct. Biol.* **2018**, *48*, 23−29. (c) Sukenik, S.; Ren, P.; Gruebele, M. Weak protein-protein interactions in live cells are quantified by cell-volume modulation. *Proc. Natl. Acad. Sci. U. S. A.* **2017**, *114* (26), 6776−6781. (d) Feng, R.; Gruebele, M.; Davis, C. M. Quantifying protein dynamics and stability in a living organism. *Nat. Commun.* **2019**, *10* (1), 1179. (e) König, I.; Zarrine-Afsar, A.; Aznauryan, M.; Soranno, A.; Wunderlich, B.; Dingfelder, F.; Stüber, J. C.; Plückthun, A.; Nettels, D.; Schuler, B. Single-molecule spectroscopy of protein conformational dynamics in live eukaryotic cells. *Nat. Methods* **2015**, *12* (8), 773−779.

(3) (a) Wang, Y.; Sarkar, M.; Smith, A. E.; Krois, A. S.; Pielak, G. J. Macromolecular Crowding and Protein Stability. *J. Am. Chem. Soc.* **2012**, *134*, 16614−16618. (b) Zimmerman, S. B.; Trach, S. O. Estimation of macromolecule concentrations and excluded volume effects for the cytoplasm of Escherichia coli. *J. Mol. Biol.* **1991**, *222* (3), 599−620.

(4) (a) Banks, D. S.; Fradin, C. Anomalous Diffusion of Proteins Due to Molecular Crowding. *Biophys. J.* **2005**, *89* (5), 2960−2971. (b) Sokolov, I. M. Models of anomalous diffusion in crowded environments. *Soft Matter* **2012**, *8* (35), 9043−9052.

(5) (a) Hong, J.; Gierasch, L. M. Macromolecular Crowding Remodels the Energy Landscape of a Protein by Favoring a More Compact Unfolded State. *J. Am. Chem. Soc.* **2010**, *132* (30), 10445−10452. (b) Soranno, A.; Koenig, I.; Borgia, M. B.; Hofmann, H.; Zosel, F.; Nettels, D.; Schuler, B. Single-molecule spectroscopy reveals polymer effects of disordered proteins in crowded environments. *Proc. Natl. Acad. Sci. U. S. A.* **2014**, *111* (13), 4874−4879.

(6) Cheung, M. S.; Klimov, D.; Thirumalai, D. Molecular crowding enhances native state stability and refolding rates of globular proteins. *Proc. Natl. Acad. Sci. U. S. A.* **2005**, *102* (13), 4753−8.

(7) (a) Minton, A. P. The effect of volume occupancy upon the thermodynamic activity of proteins: some biochemical consequences. *Mol. Cell. Biochem.* **1983**, *55* (2), 119−140. (b) Minton, A. P. Molecular crowding: analysis of effects of high concentrations of inert cosolutes on biochemical equilibria and rates in terms of volume exclusion. *Methods Enzymol.* **1998**, *295*, 127−149. (c) Zhou, H.-X. Protein folding and binding in confined spaces and in crowded solutions. *J. Mol. Recognit.* **2004**, *17* (5), 368−375.

(8) Wirth, A. J.; Gruebele, M. Quinary protein structure and the consequences of crowding in living cells: Leaving the test-tube behind. *BioEssays* **2013**, *35* (11), 984−993.

(9) (a) Mao, A. H.; Crick, S. L.; Vitalis, A.; Chicoine, C. L.; Pappu, R. V. Net charge per residue modulates conformational ensembles of intrinsically disordered proteins. *Proc. Natl. Acad. Sci. U. S. A.* **2010**, *107* (18), 8183−8188. (b) Müller-Späth, S.; Soranno, A.; Hirschfeld, V.; Hofmann, H.; Rüegger, S.; Reymond, L.; Nettels, D.; Schuler, B. Charge Interactions can Dominate the Dimensions of Intrinsically Disordered Proteins. *Proc. Natl. Acad. Sci. U. S. A.* **2010**, *107*, 14609−14614. (c) Hofmann, H.; Golbik, R.; Ott, M.; Hübner, C.; Ulbrich-Hofmann, R. Coulomb forces control the density of the collapsed unfolded state of barstar. *J. Mol. Biol.* **2008**, *376* (2), 597−605.

(10) Vancraenenbroeck, R.; Harel, Y. S.; Zheng, W.; Hofmann, H. Polymer effects modulate binding affinities in disordered proteins. *Proc. Natl. Acad. Sci. U. S. A.* **2019**, *116* (39), 19506−19512.

(11) McGuffee, S. R.; Elcock, A. H. Diffusion, crowding & protein stability in a dynamic molecular model of the bacterial cytoplasm. *PLoS Comput. Biol.* **2010**, *6* (3), No. e1000694.

(12) (a) Medina-Noyola, M.; Vizcarra-Rendón, A. Electrolyte friction and the Langevin equation for charged Brownian particles. *Phys. Rev. A: At., Mol., Opt. Phys.* **1985**, *32* (6), 3596−3605. (b) Vizcarra-Rendon, A.; Ruiz-Estrada, H.; Medina-Noyola, M.; Klein, R. Electrolyte friction on charged spherical macroparticles: Beyond the Debye-Hückel limit. *J. Chem. Phys.* **1987**, *86* (5), 2976−2985.

(13) Requiao, R. D.; Fernandes, L.; de Souza, H. J. A.; Rossetto, S.; Domitrovic, T.; Palhano, F. L. Protein charge distribution in proteomes and its impact on translation. *PLoS Comput. Biol.* **2017**, *13* (5), e1005549.

(14) Felder, C. E.; Prilusky, J.; Silman, I.; Sussman, J. L. A server and database for dipole moments of proteins. *Nucleic Acids Res.* **2007**, *35* (Web Server), W512.

(15) Gorti, S.; Ware, B. R. Probe diffusion in an aqueous polyelectrolyte solution. *J. Chem. Phys.* **1985**, *83* (12), 6449.

(16) (a) Soranno, A.; Zosel, F.; Hofmann, H. Internal friction in an intrinsically disordered protein-Comparing Rouse-like models with experiments. *J. Chem. Phys.* **2018**, *148* (12), 123326. (b) Soranno, A.; Buchli, B.; Nettels, D.; Cheng, R.; Müller-Späth, S.; Pfeil, S.; Hoffmann, A.; Lipman, E.; Makarov, D.; Schuler, B. Quantifying internal friction in unfolded and intrinsically disordered proteins with single molecule spectroscopy. *Proc. Natl. Acad. Sci. U. S. A.* **2012**, *109*, 17800−17806.

(17) Zwanzig, R. *Nonequilibrium Statistical Mechanics*; Oxford University Press: New York, 2001.

(18) Satija, R.; Das, A.; Mühle, S.; Enderlein, J.; Makarov, D. E. Kinetics of Loop Closure in Disordered Proteins: Theory vs Simulations vs Experiments. *J. Phys. Chem. B* **2020**, *124*, 3482.

(19) Brocchieri, L.; Karlin, S. Protein length in eukaryotic and prokaryotic proteomes. *Nucleic Acids Res.* **2005**, *33* (10), 3390−3400.

(20) Wilkins, D.; Grimshaw, S.; Receveur, V.; Dobson, C.; Jones, J.; Smith, L. Hydrodynamic radii of native and denatured proteins measured by pulse field gradient NMR techniques. *Biochemistry* **1999**, *38* (50), 16424−16431.

(21) Borgia, A.; Borgia, M. B.; Bugge, K.; Kissling, V. M.; Heidarsson, P. O.; Fernandes, C. B.; Sottini, A.; Soranno, A.; Buholzer, K. J.; Nettels, D.; Kragelund, B. B.; Best, R. B.; Schuler, B. Extreme disorder in an ultrahigh-affinity protein complex. *Nature* **2018**, *555* (7694), 61−66.

(22) (a) Avni, Y.; Podgornik, R.; Andelman, D. Critical behavior of charge-regulated macro-ions. *J. Chem. Phys.* **2020**, *153* (2), 024901. (b) Ninham, B. W.; Parsegian, V. A. Electrostatic potential between surfaces bearing ionizable groups in ionic equilibrium with physiologic saline solution. *J. Theor. Biol.* **1971**, *31* (3), 405−428. (c) Podgornik, R. General theory of charge regulation and surface differential capacitance. *J. Chem. Phys.* **2018**, *149* (10), 104701. (d) Frydel, D. General theory of charge regulation within the Poisson-Boltzmann framework: Study of a sticky-charged wall model. *J. Chem. Phys.* **2019**, *150* (19), 194901.

(23) Murthy, A. C.; Dignon, G. L.; Kan, Y.; Zerze, G. H.; Parekh, S. H.; Mittal, J.; Fawzi, N. L. Molecular interactions underlying liquid-liquid phase separation of the FUS low-complexity domain. *Nat. Struct. Mol. Biol.* **2019**, *26* (7), 637−648.

(24) Schuler, B.; König, I.; Soranno, A.; Nettels, D. Impact of in-cell and in-vitro crowding on the conformations and dynamics of an intrinsically disordered protein. *Angew. Chem.* **2021**, *133*, 10819.

(25) Schuler, B.; Hofmann, H. Single-molecule spectroscopy of protein folding dynamics-expanding scope and timescales. *Curr. Opin. Struct. Biol.* **2013**, *23*, 36.

(26) Kramers, H. Brownian motion in a field of force and the diffusion model of chemical reactions. *Physica* **1940**, *7*, 284−304.

(27) (a) Klimov, D. K.; Thirumalai, D. Viscosity Dependence of the Folding Rates of Proteins. *Phys. Rev. Lett.* **1997**, *79* (2), 317. (b) Wensley, B.; Batey, S.; Bone, F.; Chan, Z.; Tumelty, N.; Steward, A.; Kwa, L.; Borgia, A.; Clarke, J. Experimental evidence for a frustrated energy landscape in a three-helix-bundle protein family. *Nature* **2010**, *463* (7281), 685−U122.

(28) (a) Plaxco, K. W.; Baker, D. Limited internal friction in the rate-limiting step of a two-state protein folding reaction. *Proc. Natl. Acad. Sci. U. S. A.* **1998**, *95* (23), 13591−6. (b) Jacob, M.; Geeves, M.; Holtermann, G.; Schmid, F. X. Diffusional barrier crossing in a two-state protein folding reaction. *Nat. Struct. Biol.* **1999**, *6* (10), 923−6. (c) Jacob, M.; Schindler, T.; Balbach, J.; Schmid, F. X. Diffusion control in an elementary protein folding reaction. *Proc. Natl. Acad. Sci. U. S. A.* **1997**, *94* (11), 5622−7.

(29) (a) Ansari, A.; Jones, C. M.; Henry, E. R.; Hofrichter, J.; Eaton, W. A. The role of solvent viscosity in the dynamics of protein conformational changes. *Science* **1992**, *256* (5065), 1796−8. (b) Pabit, S. A.; Roder, H.; Hagen, S. J. Internal friction controls the speed of protein folding from a compact configuration. *Biochemistry* **2004**, *43* (39), 12532−8. (c) Hagen, S. J.; Qiu, L.; Pabit, S. A. Diffusional limits to the speed of protein folding: fact or friction? *J. Phys.: Condens. Matter* **2005**, *17* (18), S1503−S1514. (d) Cellmer, T.; Henry, E.; Hofrichter, J.; Eaton, W. Measuring internal friction of an ultrafast-folding protein. *Proc. Natl. Acad. Sci. U. S. A.* **2008**, *105*, 18320.

(30) (a) Chung, H. S.; Eaton, W. A. Single-molecule fluorescence probes dynamics of barrier crossing. *Nature* **2013**, *502* (7473), 685−688. (b) Frauenfelder, H.; Fenimore, P. W.; Chen, G.; McMahon, B. H. Protein folding is slaved to solvent motions. *Proc. Natl. Acad. Sci. U. S. A.* **2006**, *103* (42), 15469−72.

(31) (a) Evans, D. F.; Tominaga, T.; Davis, H. T. Tracer diffusion in polyatomic liquids. *J. Chem. Phys.* **1981**, *74* (2), 1298. (b) Evans, D. F.; Tominaga, T.; Chan, C. Diffusion of Symmetrical and Spherical Solutes in Protic, Aprotic, and Hydrocarbon Solvents. *J. Solution Chem.* **1979**, *8*, 461−478. (c) Pollack, G. L.; Enyeart, J. J. Atomic test of the Stokes-Einstein law. II. Diffusion of Xe through liquid hydrocarbons. *Phys. Rev. A: At., Mol., Opt. Phys.* **1985**, *31*, 980−984. (d) Hiss, T. G.; Cussler, E. L. Diffusion in high viscosity liquids. *AIChE J.* **1973**, *19*, 698−703. (e) Ellerton, H. D.; Mulcahy, D. E.; Dunlop, P. J.; Reinfelds, G. Mutual Frictional Coefficients of Several Amino Acids in Aqueous Solution at 25degree. *J. Phys. Chem.* **1964**, *68* (2), 403−408.

(32) (a) de Sancho, D.; Sirur, A.; Best, R. B. Molecular origins of internal friction effects on protein-folding rates. *Nat. Commun.* **2014**, *5*, 4307. (b) Daldrop, J. O.; Kappler, J.; Brünig, F. N.; Netz, R. R. Butane dihedral angle dynamics in water is dominated by internal friction. *Proc. Natl. Acad. Sci. U. S. A.* **2018**, *115* (20), 5169−5174.

(33) (a) Harris, K. R. The fractional Stokes-Einstein equation: Application to Lennard-Jones, molecular, and ionic liquids. *J. Chem. Phys.* **2009**, *131* (5), 054503. (b) Zwanzig, R.; Harrison, A. K. Modifications of the Stokes-Einstein Formula. *J. Chem. Phys.* **1985**, *83* (11), 5861−5862.

(34) Bhattacharyya, S.; Bagchi, B. Anomalous diffusion of small particles in dense liquids. *J. Chem. Phys.* **1997**, *106* (5), 1757−1763.

(35) (a) Grote, R. F.; Hynes, J. T. Reactive modes in condensed phase reactions. *J. Chem. Phys.* **1981**, *74*, 4465−4475. (b) Grote, R. F.; Vanderzwan, G.; Hynes, J. T. Frequency-Dependent Friction and Solution Reaction-Rates. *J. Phys. Chem.* **1984**, *88* (20), 4676−4684.

(36) Toan, N. M.; Morrison, G.; Hyeon, C.; Thirumalai, D. Kinetics of loop formation in polymer chains. *J. Phys. Chem. B* **2008**, *112* (19), 6094−6106.

(37) Cheng, R. R.; Uzawa, T.; Plaxco, K. W.; Makarov, D. E. Universality in the timescales of internal loop formation in unfolded proteins and single-stranded oligonucleotides. *Biophys. J.* **2010**, *99* (12), 3959−3968.

(38) Chandrasekhar, S. Stochastic problems in modern physics and astronomy. *Rev. Mod. Phys.* **1943**, *15*, 1−89.

(39) Zheng, W.; Zerze, G. H.; Borgia, A.; Mittal, J.; Schuler, B.; Best, R. B. Inferring properties of disordered chains from FRET transfer efficiencies. *J. Chem. Phys.* **2018**, *148* (12), 123329.

(40) Rouse, P. E. A Theory of the Linear Viscoelastic Properties of Dilute Solutions of Coiling Polymers. *J. Chem. Phys.* **1953**, *21*, 1272−1280.

(41) Barsegov, V.; Morrison, G.; Thirumalai, D. Role of internal chain dynamics on the rupture kinetic of adhesive contacts. *Phys. Rev. Lett.* **2008**, *100* (24), 248102.

(42) Makarov, D. E. Spatiotemporal correlations in denatured proteins: The dependence of fluorescence resonance energy transfer (FRET)-derived protein reconfiguration times on the location of the FRET probes. *J. Chem. Phys.* **2010**, *132* (3), 035104.

(43) (a) Adelman, S. A.; Freed, K. F. Microscopic theory of polymer internal viscosity: Mode coupling approximation for the Rouse model. *J. Chem. Phys.* **1977**, *67* (4), 1380. (b) Osaki, K.; Schrag, J. L. Viscoelastic Properties of Polymer Solutions in High-Viscosity Solvents and Limiting High-Frequency Behavior. I. Polystyrene and Poly(a-methylstyrene). *Polym. J.* **1971**, *2*, 541−549. (c) Noordermeer, J. W. M.; Kramer, O.; Nestler, M.; Schrag, J. L.; Ferry, J. D. Viscoelastic Properties of Polymer Solutions in High-Viscosity Solvents and Limiting High-Frequency Behavior. II. Branched Polystyrenes with Star and Comb···. *Macromolecules* **1975**, *8*, 539−544. (d) Noordermeer, J.; Ferry, J. D.; Nemoto, N. Viscoelastic Properties of Polymer Solutions in High-Viscosity Solvents and Limiting High-Frequency Behavior. III. Poly (2-substituted methyl acrylates). *Macromolecules* **1975**, *8*, 672−677.

(44) Allegra, G.; Ganazzoli, F. Configurations and Dynamics of Real Chains.2. Internal Viscosity. *Macromolecules* **1981**, *14* (4), 1110−1119.

(45) Elber, R.; Makarov, D. E.; Orland, H. *Molecular Kinetics in Condensed Phases: Theory, Simulation, and Analysis*; John Wiley & Sons Ltd: Hoboken, NJ, 2020.

(46) Satija, R. *Understanding Structural Transitions and Dynamics in Biomolecules at a Single Molecule Level*; University of Texas at Austin, 2020.

https://doi.org/10.1021/acs.jpcb.1c02783
J. Phys. Chem. B 2021, 125, 6144−6153